ChemComm

COMMUNICATION

View Article Online
View Journal | View Issue

Investigation of the effect of pore size on gas uptake in two fsc metal–organic frameworks†

Cite this: *Chem. Commun.*, 2014, **50**, 4911

Received 20th January 2014,
Accepted 24th March 2014

DOI: 10.1039/c4cc00477a

www.rsc.org/chemcomm

Rongming Wang,[a] Qingguo Meng,[b] Liangliang Zhang,[a] Haifeng Wang,[a] Fangna Dai,[a] Wenyue Guo,*[a] Lianming Zhao[a] and Daofeng Sun*[a]

Two porous metal–organic frameworks (1 and 2) with a fsc topology based on mixed ligands have been assembled and characterized. The different pillared ligands (pyrazine for 1 and 4,4′-bipyridine for 2) significantly influence the pore size of the frameworks. Gas uptake measurements reveal that complex 1 possesses higher H_2, CO_2, and CH_4 uptake capacities than 2, although the surface area of 1 is lower than that of complex 2. These results further experimentally prove that the pore size plays an important role in gas uptake in porous MOFs, and the slit pore with a size of ~6 Å exhibits stronger interactions with gas molecules.

Metal–organic frameworks (MOFs) built from metal-based nodes and organic polycarboxylate linkers are of enormous interest as a novel class of microporous materials due to their important applications in a wide range of fields including gas storage/separation, catalysis, nonlinear optics, electronics, and drug delivery.[1–5] Currently, design and synthesis of porous MOFs with high gas uptake capacities is still a great challenge to chemists, because many factors can influence the gas storage of an MOF. A review[6] by Yaghi summarized the strategies that can improve the hydrogen storage in an MOF, and the high porosity with an appropriate pore size, catenation, and open metal sites were thought to have a significant effect on gas uptake.

Following that, the effects of catenation and open metal sites on gas uptake capacities of an MOF have been experimentally and theoretically studied. In particular, Zhou and coworkers systematically studied the effect of catenation on the gas uptake of porous MOFs and concluded that catenated porous frameworks possess higher gas uptake capacities than noncatenated ones at low pressure and 77 K.[7] Similar results were also observed in MOFs of the IRMOF-series.[8] Several other research groups have also proven that open metal sites have a significant effect on gas storage of an MOF and can improve the gas uptake dramatically.[9–11] It has been calculated based on carbon materials that the ideal pore size for maximal attraction of H_2 molecules is ~6 Å at low pressure because these pores exhibit the strongest interaction potential with H_2 molecules.[12] For porous MOFs, neutron powder diffraction and inelastic neutron scattering (INS) studies[13] on HKUST-1 reveal that H_2 molecules are adsorbed in the smaller cages before the larger ones, indicating the higher affinity of the smaller pores for H_2 molecules.[14] However, there is no experimentally systematic comparison or investigation of the effect of pore size on gas uptake in porous MOFs with similar structures. Very recently, Zaworotko and coworkers reported a crystal engineering strategy that can improve CO_2 uptake and sorption selectivity through controlling the pore functionality and size.[15] The effect of pore size on gas selectivity was observed in their study.

In this communication, we report two porous metal–organic frameworks, $Co(pz)(BPTC)_{0.5}\cdot dmf\cdot EtOH\cdot 4H_2O$ (**1**) and $Co(bipy)(BPTC)_{0.5}\cdot$solvent (**2**) ($H_4BPTC$ = 3,3′,5,5′-biphenyltetracarboxylate, pz = pyrazine, bipy = 4,4′-bipyridine), with a **fsc** topology based on mixed ligands (Scheme 1). Both **1** and **2** are based on 2D $Co(BPTC)_{0.5}$ layers, which are further connected by pz or bipy as pillars to generate 3D porous frameworks with similar channels but different pore sizes. The investigation and systematic comparison of the effect of pore size on gas uptake have also been carried out.

1 and **2** were synthesized by the solvothermal reaction of $Co(NO_3)_2$, H_4BPTC and pz or bipy in mixed dmf/EtOH/H_2O solvents, and structurally characterized by single-crystal X-ray crystallography, powder X-ray diffraction (PXRD), thermogravimetric analysis (TGA), and elemental analysis. Single-crystal X-ray diffraction reveals that **1** and **2** possess 3D pillared frameworks with a **fsc** topology based on the binuclear SBU. Complex **1** crystallizes in the orthorhombic *Pbam* space group and the asymmetric unit consists of 0.5 cobalt ion, 0.25 BPTC ligand, and 0.5 pz ligand, whereas complex **2** crystallizes in the monoclinic $P2_1/c$ space group and the asymmetric unit consists

[a] *State Key Laboratory of Heavy Oil Processing, China University of Petroleum (East China), College of Science, China University of Petroleum (East China), Qingdao, Shandong 266580, People's Republic of China. E-mail: dfsun@upc.edu.cn, wyguo@upc.edu.cn*

[b] *Chemistry & Chemical and Environmental Engineering College, Weifang University, Weifang 261061, China*

† Electronic supplementary information (ESI) available: Synthesis, crystallographic information, TGA, XRD pattern. CCDC 981845 and 981846. For ESI and crystallographic data in CIF or other electronic format see DOI: 10.1039/c4cc00477a

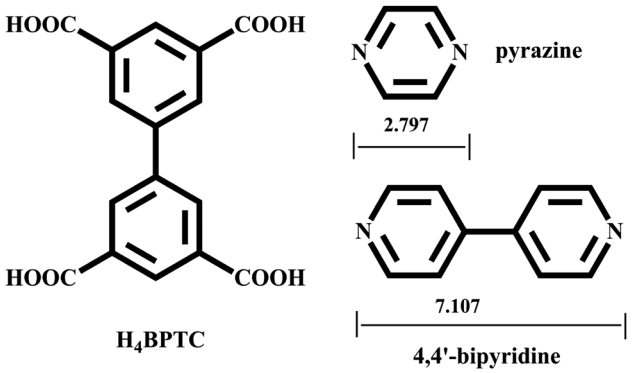

Scheme 1 (left) Tetracarboxylate ligand for connecting metal ions to form layers, and (right) the pillars for controlling the pore size in this work.

of one cobalt ion, 0.5 BPTC ligand, and one bipy ligand. In **1** and **2**, the central cobalt ion is six-coordinated by four oxygen atoms from two BPTC ligands and two nitrogen atoms from two pillared ligands (pz or bipy), in a distorted octahedral geometry. Two cobalt ions are engaged by two carboxylate groups to generate a binuclear $Co(COO)_2$ unit (Fig. 1a and b), which is further linked by the backbone of BPTC ligands in the *ab* plane to form a 2D layer (Fig. 1c). If the BPTC ligand and the binuclear unit can be considered as planar 4-connected nodes, then the 2D layer is a (4,4) net. The 2D layers are further double-pillared by pz or bipy along the *c* axis to generate 3D porous frameworks. For the whole framework, if the binuclear SBU can be simplified as a six-connected node, the BPTC ligand as a planar 4-connected node and pz or bipy as a linear linker, then the whole framework possesses a **fsc** topology (Fig. 1d).

The purity of **1** and **2** was confirmed by comparison of their simulated and experimental powder X-ray diffraction patterns. As analyzed by single-crystal X-ray diffraction, **1** and **2** are open frameworks with 1D channels along [110] and [011] directions,

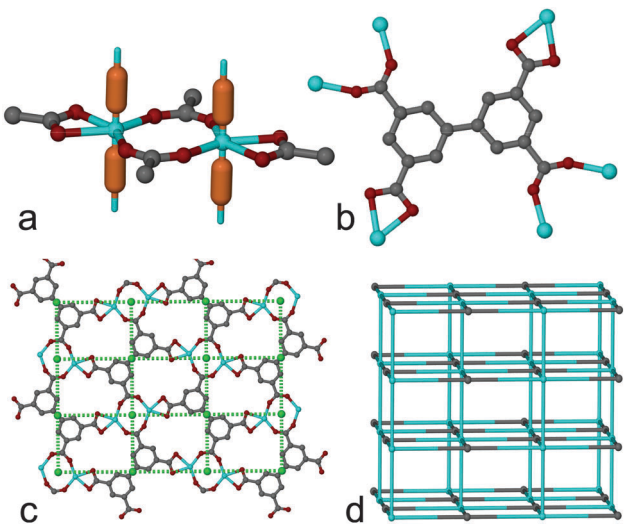

Fig. 1 (a) The binuclear SBU, the brown linkers represent the pillars such as pz or bipy, (b) the coordination mode of the BPTC ligand, (c) the (4,4) layer, and (d) the **fsc** topology with the gray and green balls representing the planar 4-connected node (BPTC ligand) and the 6-connected node (SBU), respectively.

Table 1 Comparison of porosities, pore volumes, surface areas, and Q_{st}'s of **1** and **2**

	1	**2**
Porosity[a]	38.5%	50.5%
Pore volume ($cm^3\ g^{-1}$)	0.95	1.31
Surface area ($m^2\ g^{-1}$)	703	870
Q_{st} for H_2 (kJ mol^{-1})	8.7	7.5
Q_{st} for CH_4 (kJ mol^{-1})	17.5	13.5
Q_{st} for CO_2 (kJ mol^{-1})	27	10

[a] Calculated using PLATON.[16]

respectively. The dimensions of the channels are 6.519 × 7.105 Å and 6.555 × 11.399 Å, respectively. The solvent-accessible volumes calculated by PLATON[16] are 630.5 and 1328.3 $Å^3$, corresponding to 38.5 and 50.5% of unit cells of **1** and **2**, respectively (Table 1). To check the permanent porosities of complexes **1** and **2**, the freshly prepared samples were soaked in methanol and dichloromethane to exchange the less volatile solvents, followed by evacuation under a dynamic vacuum at 80 °C for 10 h, generating dehydrated forms. The adsorption equilibrium data of N_2, H_2, CH_4, and CO_2 were collected, and to our surprise, **1** and **2** showed extraordinary gas uptake, and the aperture effect on **1** and **2** was studied in this work.

As shown in Fig. 2, desolvated **1** and **2** display typical type-I adsorption isotherms, suggesting the retention of the microporous structures after the removal of solvents from the crystalline samples. Both sets of isotherms show slight changes in slopes between 0.01 to 0.1 bar, indicating that the different sized pores are filled in a sequence as the pressure increases from below 0.01 to 0.1 bar. Desolvated **1** and **2** adsorb 173 and 221 $cm^3\ g^{-1}$ of N_2 at 77 K, respectively. The total pore volumes of 0.95 and 1.31 $cm^3\ g^{-1}$ for **1** and **2**, respectively, were calculated from the N_2 isotherms (P/P_0 = 0.98). The Brunauer–Emmett–Teller (BET) surface areas by fitting the N_2 isotherms are 703 and 870 $m^2\ g^{-1}$ for **1** and **2**, respectively, showing good agreement with the crystal structures as well as the solvent-accessible volumes calculated by PLATON.[16]

Although complex **2** possesses a higher BET surface area and pore volume compared to **1**, H_2, CH_4, and CO_2 measurements for **1** and **2** show extraordinary results. Low-pressure H_2, CH_4, and CO_2 uptake capacities of desolvated samples of **1** and **2**

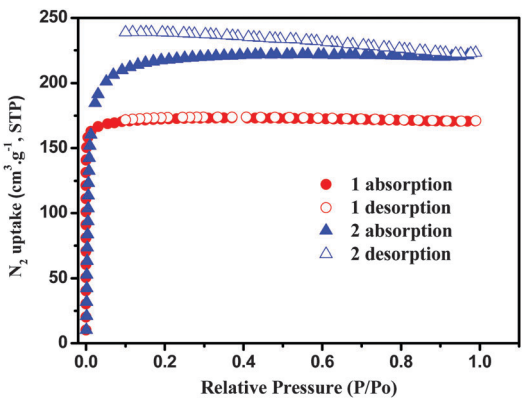

Fig. 2 The N_2 sorption isotherms at 77 K for **1** and **2**.

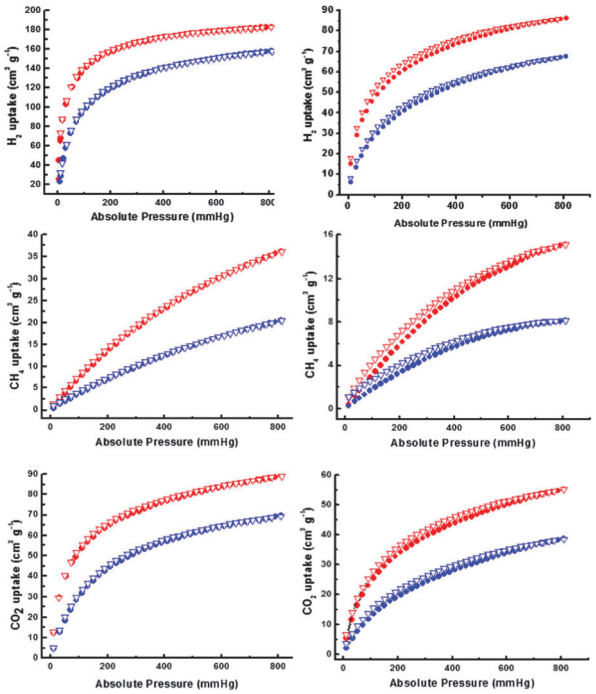

Fig. 3 The H_2, CH_4, and CO_2 sorption isotherms for **1** (left) and **2** (right). H_2: red, 77 K; blue, 87 K. CH_4: red, 273 K; blue, 300 K. CO_2: red, 273 K; blue, 300 K.

were continuously determined using volumetric gas adsorption measurements. As shown in Fig. 3, desolvated **1** and **2** exhibit the classical reversible type-I isotherms for H_2, CH_4, and CO_2. Under the conditions of 77 K and **1** bar, desolvated **1** and **2** exhibit quite different H_2 uptake capacities, 182 $cm^3\ g^{-1}$ for **1** and 46 $cm^3\ g^{-1}$ for **2**, respectively. The H_2 isosteric heat of adsorption (Q_{st}) for **1** and **2** was calculated by fitting the H_2 adsorption isotherms at 77 K and 87 K to a virial-type expression. At the lowest coverage, the Q_{st} has the estimated values of 8.7 and 7.5 kJ mol^{-1} for **1** and **2** (Fig. 4), respectively, indicating that the framework of **1** possesses higher affinity for H_2 molecules than that of **2**. Similar results were obtained for CH_4 and CO_2 uptakes in **1** and **2**. Both **1** and **2** possess low CH_4

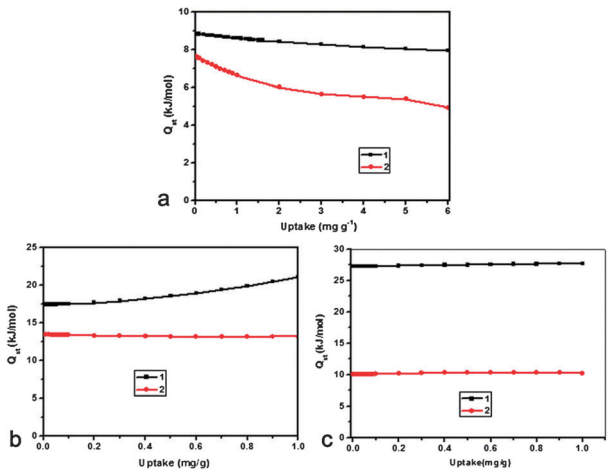

Fig. 4 The Q_{st}'s of **1** and **2** for H_2, CH_4, and CO_2.

uptake capacities at 298 K with the total adsorption amounts of 36 and 15 $cm^3\ g^{-1}$ for **1** and **2**, respectively. The corresponding Q_{st} values calculated by fitting the CH_4 adsorption isotherms at 273 K and 298 K to a virial-type expression are 17.5 and 13.5 for **1** and **2**, respectively. For CO_2 uptake, **1** and **2** can adsorb 89 and 55 $cm^3\ g^{-1}$, respectively, at 273 K and **1** bar. Complex **1** exhibits a Q_{st} of $\sim$27.0 kJ mol^{-1} at zero-loading, which is 17 kJ mol^{-1} higher than that of **2** (Q_{st} of 10 kJ mol^{-1}), indicating that complex **1** possesses high affinity for CO_2 molecules. The value of Q_{st} of CO_2 for **1** is comparable to that of the PAF-1/C-900 material,[17] which possesses a pore size similar to that of **1**.

It is well known that there is no linear relationship between the surface area and gas uptake for an MOF at low pressure, which indicates that there are a lot of other factors that can influence gas uptake besides the surface area.[18] In our work, complex **2** possesses a higher surface area, but lower H_2, CH_4, and CO_2 uptake capacities and the corresponding Q_{st} values than those of **1**. These results make us re-analyse the crystal structures of **1** and **2**. Both **1** and **2** are pillared frameworks with a (4,6)-connected **fsc** topology. The only difference between **1** and **2** is the length of the pillars, pz for **1** and bipy for **2**. As shown in Fig. 5, there exist hexahedral boxes made up of four double-pillars and two BPTC ligands in **1** and **2**. Due to the different lengths of the pillars, the sizes of the boxes are distinct, 6.519 × 7.105 Å for **1** and 6.555 × 11.399 Å for **2**, respectively, which are equal to the sizes of the channels along [110] and [011] directions for **1** and **2**, respectively. It has been calculated based on carbon materials that a slit pore with a size of 6 Å possesses the highest hydrogen uptake at very low pressure because it exhibits the strongest interaction potential with the wall of the material. Thus, the porous framework of **1** exhibits a suitable pore size that can match the kinetic diameter of hydrogen (2.9 Å) better than that of **2**. These results prove that the hexahedral boxes of **1** exhibit stronger interactions with H_2 molecules than those of **2**, further proving that complex **1** possesses much higher hydrogen uptake (182 $cm^3\ g^{-1}$ *vs.* 46 $cm^3\ g^{-1}$) than **2**. Similarly, the CH_4 and CO_2 uptake capacities of complex **1** are much higher than those of **2**, which can also be ascribed to the influence of aperture effect. In the past decade, although several MOFs with a **fsc** topology have been reported,[19] only a few have been studied for their gas uptake, especially observing the effect of pore size on gas adsorption capacity.

In conclusion, two pillared cobalt–organic frameworks (**1** and **2**) with a **fsc** topology based on mixed ligands have been assembled and characterized. The different lengths of the pillars lead to **1** and **2** possessing different pore sizes (6.519 × 7.105 Å *vs.* 6.555 × 11.399 Å). Complex **1** exhibits a lower surface area, but

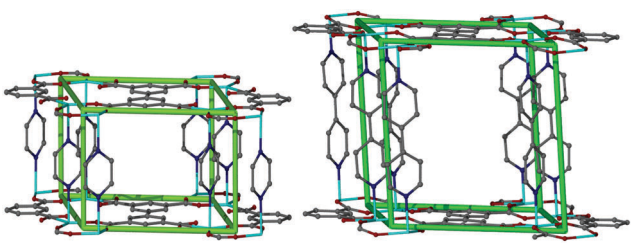

Fig. 5 The hexahedral boxes existed in **1** (left) and **2** (right) with the pore sizes of 6.519 × 7.105 Å and 6.555 × 11.399 Å, respectively.

higher H_2, CH_4, and CO_2 uptake capacities compared to complex **2**. These gas uptake results reveal that complex **1** possesses higher affinity for gas molecules compared to **2** due to the existence of hexahedral boxes with a suitable pore size (aperture effect). Our results presented here may further experimentally prove that a slit pore with a size of ~6 Å exhibits stronger interaction potential with gas molecules, and provide a strategy that can improve the gas uptake capacities in designing porous MOFs in the future.

This work was financially supported by the NSFC (Grant No. 21271117, 21371179), NCET-11-0309, the Shandong Natural Science Fund for Distinguished Young Scholars (JQ201003), NSF of Shandong Province (BS2011CL041), the Shandong Provincial Natural Science Foundation (ZR2010BL011), and the Fundamental Research Funds for the Central Universities (13CX05010A, 13CX02006A).

Notes and references

1 For recent reviews, see: (*a*) H.–C. Zhou, J. R. Long and O. M. Yaghi, *Chem. Rev.*, 2012, **112**, 673; (*b*) K. Sumida, D. L. Rogow, J. A. Mason, T. M. McDonald, E. D. Bloch, Z. R. Herm, T. H. Bae and J. R. Long, *Chem. Rev.*, 2012, **112**, 724; (*c*) M. P. Suh, H. J. Park, T. K. Prasad and D. W. Lim, *Chem. Rev.*, 2012, **112**, 782; (*d*) J. R. Li, J. Sculley and H.–C. Zhou, *Chem. Rev.*, 2012, **112**, 869; (*e*) C. Wang, T. Zhang and W. B. Lin, *Chem. Rev.*, 2012, **112**, 1084; (*f*) Y. J. Cui, Y. F. Yue, G. D. Qian and B. L. Chen, *Chem. Rev.*, 2012, **112**, 1126; (*g*) M. Yoon, R. Srirambalaji and K. Kim, *Chem. Rev.*, 2012, **112**, 1196.

2 (*a*) A. Schoedel, W. Boyette, L. Wojtas, M. Eddaoudi and M. J. Zaworotko, *J. Am. Chem. Soc.*, 2013, **135**, 14016; (*b*) P. Deria, J. E. Mondloch, E. Tylianakis, P. Ghosh, W. Bury, R. Q. Snurr, J. T. Hupp and O. K. Farha, *J. Am. Chem. Soc.*, 2013, **135**, 16801; (*c*) R. Q. Zou, H. Sakurai, S. Han, R. Q. Zhong and Q. Xu, *J. Am. Chem. Soc.*, 2007, **129**, 8402; (*d*) Y. Liu, G. Li, X. Li and Y. Cui, *Angew. Chem., Int. Ed.*, 2007, **46**, 6301.

3 (*a*) G. Ferey, C. Mellot-Draznieks, C. Serre, F. Millange, J. Dutour, S. Surble and I. Margiolaki, *Science*, 2005, **309**, 2040; (*b*) E. D. Bloch, W. L. Queen, R. Krishna, J. M. Zadrozny, C. M. Brown and J. R. Long, *Science*, 2012, **335**, 1606; (*c*) H. X. Deng, S. Grunder, K. E. Cordova, C. Valente, H. Furukawa, M. Hmadeh, F. Gandara, A. C. Whalley, Z. Liu, S. Asahina, H. Kazumori, M. O'Keeffe, O. Terasaki, J. F. Stoddart and O. M. Yaghi, *Science*, 2012, **336**, 1018.

4 (*a*) J. A. Mason, K. Sumida, Z. R. Herm, R. Krishna and J. R. Long, *Energy Environ. Sci.*, 2011, **4**, 3030; (*b*) N. R. Champness, *Dalton Trans.*, 2011, **40**, 10311; (*c*) Y. B. He, W. Zhou, R. Krishna and B. L. Chen, *Chem. Commun.*, 2012, **48**, 11813; (*d*) J. J. Qian, F. L. Jiang, D. Q. Yuan, X. J. Li, L. J. Zhang, K. Z. Su and M. C. Hong, *J. Mater. Chem. A*, 2013, **1**, 9075; (*e*) L. T. Du, Z. Y. Lu, K. Y. Zheng, J. Y. Wang, X. Zheng, Y. Pan, X. Z. You and J. F. Bai, *J. Am. Chem. Soc.*, 2013, **135**, 562.

5 (*a*) G. Lu, S. Li, Z. Guo, O. K. Farha, B. G. Hauser, X. Qi, Y. Wang, X. Wang, S. Han, X. Liu, J. S. DuChene, H. Zhang, Q. Zhang, X. Chen, J. Ma, S. C. Loo, W. D. Wei, Y. Yang, J. T. Hupp and F. Huo, *Nat. Chem.*, 2012, **4**, 310; (*b*) X. Lin, J. Jia, X. Zhao, K. M. Thomas, A. J. Blake, G. S. Walker, N. R. Champness, P. Hubberstey and M. Schroder, *Angew. Chem., Int. Ed.*, 2006, **45**, 7358; (*c*) B. Li, Z. Zhang, Y. Li, K. Yao, Y. Zhu, Z. Deng, F. Yang, X. Zhou, G. Li, H. Wu, N. Nijem, Y. J. Chabal, Z. Lai, Y. Han, Z. Shi, S. Feng and J. Li, *Angew. Chem., Int. Ed.*, 2012, **51**, 1412; (*d*) B. Zheng, J. Bai, J. Duan, L. Wojtas and M. J. Zaworotko, *J. Am. Chem. Soc.*, 2011, **133**, 748.

6 J. L. C. Rowsell and O. M. Yaghi, *Angew. Chem., Int. Ed.*, 2005, **44**, 4670.

7 S. Ma, J. Eckert, P. M. Forster, J. W. Yoon, Y. K. Hwang, J. S. Chang, C. D. Collier, J. B. Parise and H.–C. Zhou, *J. Am. Chem. Soc.*, 2008, **130**, 15896.

8 (*a*) J. L. C. Rowsell and O. M. Yaghi, *J. Am. Chem. Soc.*, 2006, **128**, 1304; (*b*) D. H. Jung, D. Kim, T. B. Lee, S. B. Choi, J. H. Yoon, J. Kim, K. Choi and S. H. Choi, *J. Phys. Chem. B*, 2006, **110**, 22987.

9 Y. Yan, S. H. Yang, A. J. Blake and M. Schroder, *Acc. Chem. Res.*, 2014, **47**, 296.

10 (*a*) K. L. Mulfort, O. K. Farha, C. L. Stern, A. A. Sarjeant and J. T. Hupp, *J. Am. Chem. Soc.*, 2009, **131**, 3866; (*b*) N. Nijem, J. F. Veyan, L. Z. Kong, H. Wu, Y. G. Zhao, J. Li, D. C. Langreth and Y. J. Chabal, *J. Am. Chem. Soc.*, 2010, **132**, 14834; (*c*) H. Wu, W. Zhou and T. Yildirim, *J. Am. Chem. Soc.*, 2009, **131**, 4995; (*d*) Y. Y. Fu, C. X. Yang and X. P. Yan, *Langmuir*, 2012, **28**, 6794.

11 (*a*) Q. Y. Yang and C. L. Zhong, *J. Phys. Chem. B*, 2006, **110**, 655; (*b*) Y. Y. Sun, Y. H. Kim and S. B. Zhang, *J. Am. Chem. Soc.*, 2007, **129**, 12606; (*c*) W. Zhou and T. Yildirim, *J. Phys. Chem. C*, 2008, **112**, 8132.

12 Q. Y. Wang and J. K. Johnson, *J. Chem. Phys.*, 1999, **110**, 577.

13 (*a*) V. K. Peterson, Y. Liu, C. M. Brown and C. J. Kepert, *J. Am. Chem. Soc.*, 2006, **128**, 15578; (*b*) Y. Liu, C. M. Brown, D. A. Neumann, V. K. Peterson and C. J. Kepert, *J. Alloys Compd.*, 2007, **446**, 385.

14 (*a*) B. Panella, K. Hones, U. Muller, N. Trukhan, M. Schubert, H. Putter and M. Hirscher, *Angew. Chem., Int. Ed.*, 2008, **47**, 2138; (*b*) O. K. Farha, A. M. Spokoyny, K. L. Mulfort, M. F. Hawthorne, C. A. Mirkin and J. T. Hupp, *J. Am. Chem. Soc.*, 2007, **129**, 12680; (*c*) L. Pan, M. B. Sander, X. Y. Huang, J. Li, M. Smith, E. Bittner, B. Bockrath and J. K. Johnson, *J. Am. Chem. Soc.*, 2004, **126**, 1308.

15 P. Nugent, Y. Belmabkhout, S. D. Burd, A. J. Cairns, R. Luebke, K. Forrest, T. Pham, S. Q. Ma, B. Space, L. Wojtas, M. Eddaoudi and M. J. Zaworotko, *Nature*, 2013, **495**, 80.

16 A. L. Spek, *J. Appl. Crystallogr.*, 2003, **36**, 7.

17 Y. M. Zhang, B. Y. Li, K. Williams, W. Y. Gao and S. Q. Ma, *Chem. Commun.*, 2013, **49**, 10269.

18 D. Zhao, D. Q. Yuan and H.–C. Zhou, *Energy Environ. Sci.*, 2008, **1**, 222.

19 (*a*) M. H. Bi, G. H. Li, J. Hua, Y. L. Liu, X. M. Liu, Y. W. Hu, Z. Shi and S. H. Feng, *Cryst. Growth Des.*, 2007, **7**, 2066; (*b*) L. K. Sposato, J. H. Nettleman, M. A. Braverman, R. M. Supkowski and R. L. LaDuca, *Cryst. Growth Des.*, 2010, **10**, 335; (*c*) D. C. Zhong, W. G. Lu, L. Jiang, X. L. Feng and T. B. Lu, *Cryst. Growth Des.*, 2010, **10**, 739.

